Structural geology of the eastern Richardson Mountains, Yukon and Northwest Territories: Some field observations and a note of caution for palinspastic reconstructions

Nicolas Pinet
Natural Resources Canada, Geological Survey of Canada

Pinet, N., 2021. Structural geology of the eastern Richardson Mountains, Yukon and Northwest Territories: Some field observations and a note of caution for palinspastic reconstructions. *In:* Yukon Exploration and Geology 2020, K.E. MacFarlane (ed.), Yukon Geological Survey, p. 1–18.

Abstract

The Richardson anticlinorium is a major tectonic feature marking the eastern limit of the Cordilleran orogen in northern Yukon and Northwest Territories. Limited structural observations on the eastern flank of the Richardson anticlinorium indicate that the strain intensity increases significantly close to major faults that are associated with deformation zones tens to hundreds of metres wide. A predominant dextral sense of motion is documented for several major faults belonging to the Richardson fault array. However, second-order features exhibit highly variable kinematics. In several cases, strike-slip faults cut shallower dipping faults and follow steep bedding planes, suggesting that dextral motion occurred in a previously deformed and tilted sedimentary succession. The amount of displacement along the Richardson fault array is poorly constrained. Further investigation is warranted as potential large displacements may bear significant consequences on palinspastic reconstructions.

* nicolas.pinet@canada.ca

Introduction

Paleogeographic reconstructions need an appraisal of post-sedimentation deformation as major faults may have juxtaposed rock units originating from different sedimentary environments. However, early studies in frontier sedimentary basins generally focused on stratigraphic and sedimentologic analyses in order to build a regional-scale geological framework. At the reconnaissance stage, tectonic features are often implicitly considered as second-order importance for regional-scale basin reconstructions.

In 1961, the Geological Survey of Canada (GSC) initiated a large-scale geological mapping study, Operation Porcupine, that has described a thick Proterozoic to Tertiary sedimentary succession in northern Yukon and Northwest Territories. Facies changes in strata have been documented for both Paleozoic (Norford, 1996; Morrow, 1999) and Mesozoic (Dixon, 1996). These facies changes reflect paleogeographic features such as uplifts and troughs extending for tens to hundreds kilometres.

The aim of this paper is to report structural observations from the eastern Richardson Mountains. Despite uncertain offset along major structures, it is argued that displacement along the Richardson fault array should be kept in mind for palinspastic reconstructions.

Geological Framework

The Richardson Mountains mark the eastern limit of the Cordilleran orogen (Fig. 1), and corresponds to the north-northwest trending Richardson anticlinorium, which is up to 75 km in width. The Richardson anticlinorium is a north-plunging structure that includes deformed Proterozoic to Carboniferous rock units. It is bounded by generally flat to shallow-dipping strata of the Peel Plateau and Eagle Plain to the east and west of the anticlinorium respectively. To the south, the Richardson Mountains terminate at the east-west trending Ogilvie, Wernecke and Mackenzie mountains.

The sedimentary succession preserved in the Richardson anticlinorium consists of Cambrian to Early Devonian sediments deposited in water deeper than surrounding areas. This led several authors to interpret that the Paleozoic rocks of the Richardson Mountains were deposited in an elongated basin, approximately perpendicular to the northern continental margin (Richardson trough or aulacogen; Norris and Yorath, 1981; Pugh, 1983; Fraser and Hutchison, 2017; Strauss *et al.*, 2020).

Tectonic slivers of Proterozoic rocks constitute the oldest unit of the Richardson anticlinorium. In the central part the anticlinorium, the base of the exposed Paleozoic succession consists of a limestone unit (Ittlyd Formation) and a clastic-dominated assemblage (Slats Creek Formation). Predominantly fine-grained carbonate and siliciclastic strata of the Road River Group overlie this assemblage and include four recently formalized formations: from base up are the Cronin, Mount Hare, Tetlit and Vittrekwa formations (Strauss *et al.*, 2020). The black siliceous shale of the Canol Formation overlies the Road River Group as well as coeval rocks found in the Eagle Plain and Peel Plateau, and represents a regional marker interval (Fraser and Hutchison, 2017). The Canol Formation is conformably overlain by the Upper Devonian Imperial Formation, a thick sequence of predominantly mudstone and shale in its basal section, with more sandstone higher up in the succession (Allen, 2009; Fraser and Hutchison, 2017). On both sides of the anticlinorium, lower and middle Paleozoic strata are overlain by, or in fault contact with, upper Paleozoic and Mesozoic unconformity bounded rock assemblages.

The Richardson anticlinorium is cut by the Richardson fault array (RFA; Norris and Hopkins, 1977), a series of north-trending faults that extend from the Mackenzie Mountains to the Arctic Ocean. To the north, the RFA probably continues across the continental margin to connect with the Taglu and/or Eskimo Lakes fault zones (Lane, 1998), extending its total length to approximately 1000 km (Norris, 1996).

The Trevor and Deception faults, both part of the Richardson fault array, bound the Richardson anticlinorium to the east and west, respectively (Fig. 2). The RFA is seismically the most active structure in northern Yukon and Northwest Territories (Mazotti and Hyndman, 2002).

Kinematic interpretation of the RFA varies significantly in the literature. Norris and Yorath (1981) consider displacement by the RFA as dextral, while Eisbacher (1983) interprets it as sinistral. Alternatively, Norris (1985) indicates the RFA is experiencing mainly differential vertical motion during the early to mid-Tertiary, while Cecile (1984) considers a relatively minor (10 km or less) strike-slip motion.

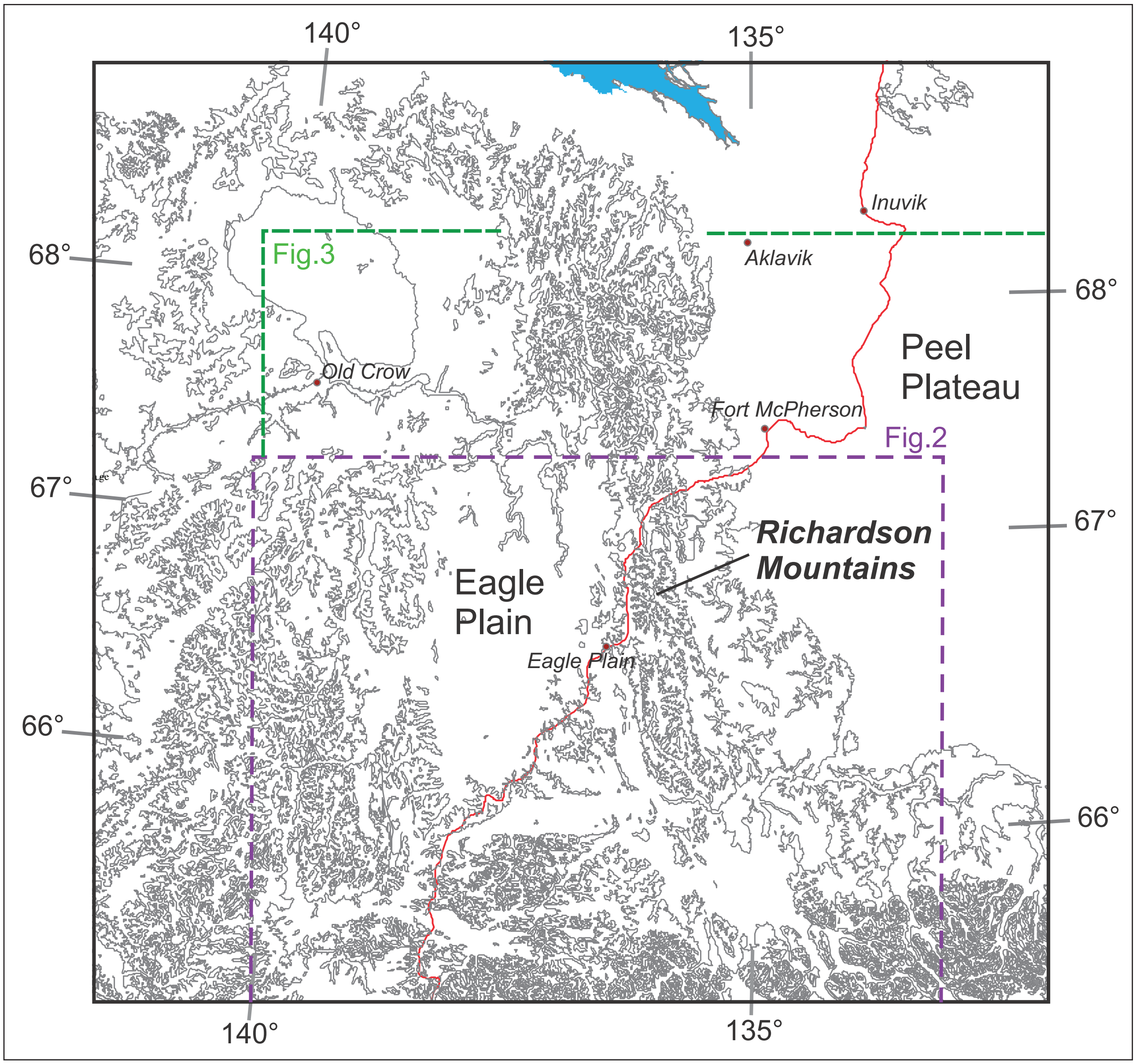

Figure 1. *Physiographic framework of the Richardson Mountains. The red line indicates the Dempster Highway.*

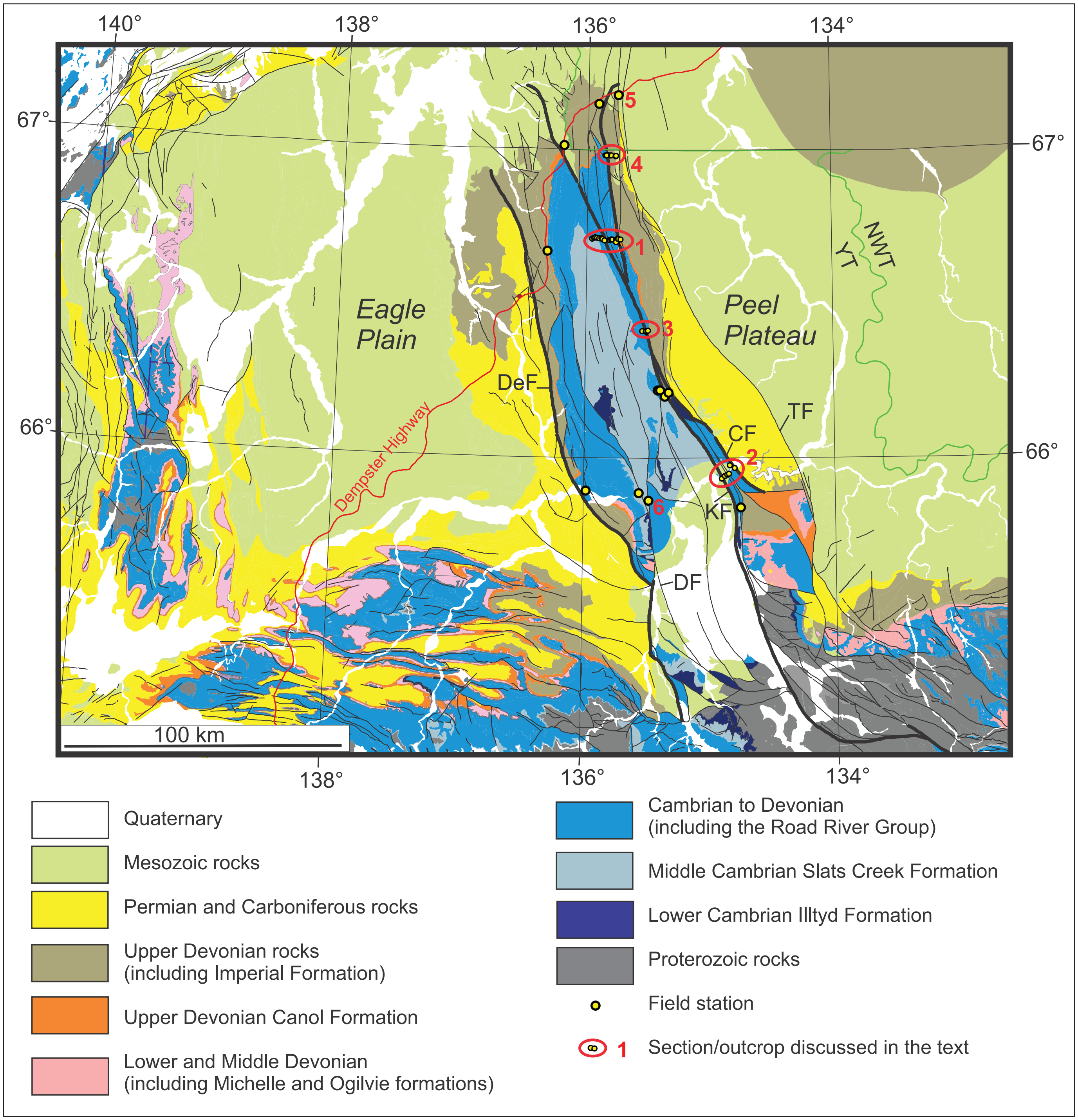

Figure 2. *Geological map of the Richardson Mountains and adjacent Eagle Plain and Peel Plateau (adapted from Norris 1981a to d). CF = Caribou fault; DF = Deslauriers fault; DeF = Deception fault; KF = Knorr fault; TF = Trevor fault; NWT = Northwest Territories; YT = Yukon; 1 = Tetlit River section; 2 = eastern Peel River section; 3=Trail River section; 4 = Vittrekwa River; 5 = Dempster Highway; 6 = western Peel River.*

Geophysical Framework

Fair to good quality seismic data are available for the Eagle Plain and Peel Plateau on both sides of the Richardson anticlinorium. These hydrocarbon exploration seismic lines generally end at the Richardson Mountains (Osadetz *et al.*, 2005; Rohr *et al.*, 2011) and the geometry of the anticlinorium is therefore poorly constrained. Based on the available seismic data set, Hall and Cook (1998) interpreted the Richardson anticlinorium as a pop-up structure formed above a regional detachment that extends westward beneath Eagle Plain.

A positive Bouguer gravity anomaly is centred on the Richardson anticlinorium (Fig. 3a). Gradients greater than 1 mGal/km characterize the east side of the anticlinorium. The boundaries of the gravity anomaly are enhanced on the map of the horizontal gradient of the Bouguer anomaly, and are almost coincident with mapped faults (Fig. 3b). As noted by Hall and Cook (1998), this anomaly probably reflects the presence of high-density Precambrian rocks in the core of the anticlinorium.

On the map of the residual total magnetic field, the RFA also corresponds to a clear boundary between domains with different long-wavelength anomaly signatures (Crawford et *al.*, 2010).

Structural Analysis

Structural observations were collected during the 2010 field season and precede the recent clarification of the Road River Group stratigraphy (Strauss et *al.*, 2020). For this reason, the recently formalized formations are not used in the following descriptions.

Tetlit section

A nearly continuous section of the east flank of the Richardson Mountains (Fig. 4; location 1 on Fig. 2) is found along the Tetlit River. Structural repetition of Canol Formation and part of the Imperial Formation occurs at this section.

Rock units dip almost invariably toward the east. The dips are generally shallow (<30°) except close to fault zones where bedding is steep (70 to 90°). Exposure of two main fault zones along the Tetlit River are informally referred to as the east and west Tetlit fault zones. On the published geological map, they correspond to fault splays of the Knorr fault (Norris, 1981c).

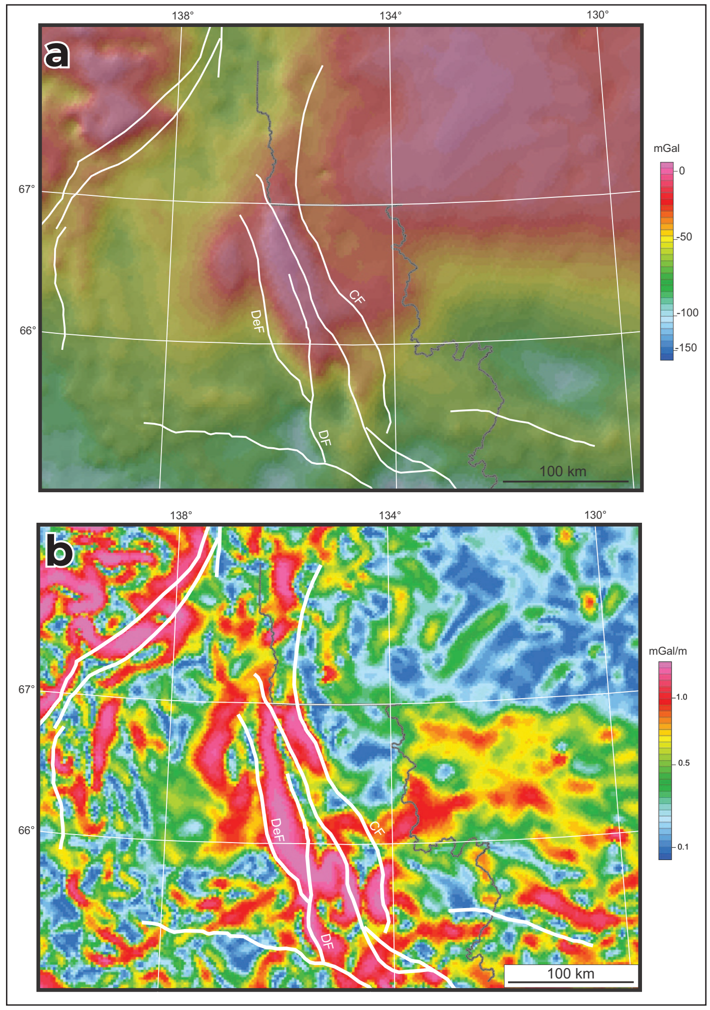

Figure 3. *Gravity maps of the Richardson Mountains and adjacent areas.* ***(a)*** *Bouguer anomaly map and* ***(b)*** *horizontal derivative of the Bouguer anomaly. White lines indicate main faults: CF = Caribou fault; DF = Deslauriers fault; DeF = Deception fault.*

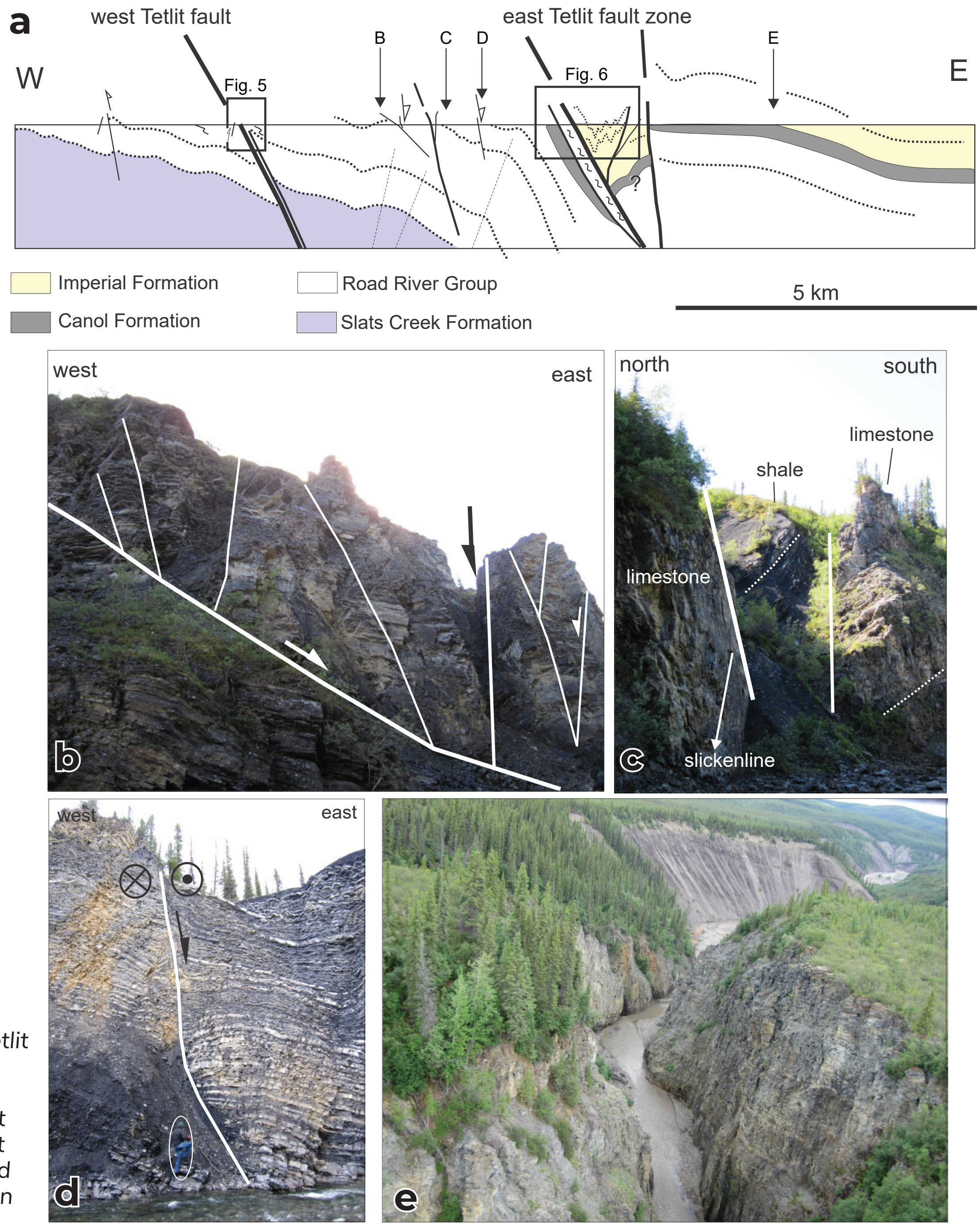

Figure 4. (a) *Cross section along the Tetlit River (location 1 on Fig. 2); no vertical exaggeration. Offset along the west Tetlit fault is unknown and shown for illustration purposes only. The eastern part of the section has not been studied in detail and the geometry of the Imperial Formation is based on a helicopter reconnaissance survey and on the study of Allen (2009). Locations for 4b to e indicated on section.* **(b)** *Brittle faults showing predominant normal motion, with a minor right-lateral component. Offsets along high angle faults are generally less than 1 m. Offset along shallow dipping fault is unknown. The width of the section pictured is approximately 20 m.* **(c)** *Brittle faults juxtaposing a shale-dominated unit against a limestone. A 5 m wide brecciated zone characterizes the main fault. The pitch of slickenlines found on the main fault plane is 45° suggesting that both the horizontal and vertical components of motion are significant. However, the sense of motion is unclear. The width of the section pictured is around 15 m. Dotted lines represent the bedding.* **(d)** *Brittle fault showing mixed right-lateral and normal motion. Geologist for scale (outlined by white oval).* **(e)** *Aerial view looking east, showing the contact between the Canol Formation (foreground) and the Imperial Formation (back).*

The east Tetlit fault zone marks the contact between a siltstone-dominated assemblage to the west and a limestone-dominated assemblage to the east, both belonging to the Road River Group. The fault trends N350 and is marked by a 4 m wide schistose zone (Fig. 5a) and a 120 m wide brecciated zone. Within the schistose zone, slickenlines on fault planes indicate predominant strike-slip motion (Fig. 5b) with an uncertain sense of slip. The brecciated zone corresponds to a cohesive tectonic breccia that contains centimetre to decimetre long angular fragments in a matrix formed by crushed rocks (Fig. 5c). Calcite veinlets and fractures (with a predominant N150 strike) are common in the brecciated zone.

The west Tetlit fault zone corresponds to a kilometre-wide deformation zone (Figs. 4 and 6). West of the main deformation zone, the contact between the shale-dominated upper part of the Road River Group and the Canol Formation dips steeply (70°) to the east. Within the Canol Formation, second-order faults associated with metre-thick cataclastic zones record predominantly right-lateral motions (Fig. 6a,b,c). The main zone of deformation is several hundred metres wide. It occurs in a fine-grained assemblage that includes fault bounded, elongated, competent blocks up to tens of metres in length (Fig. 6d,e). In a number of locations, several disconnected blocks are aligned with a plane parallel to bedding. The blocks are brecciated and bounded by deformed zones delineated by a scaly fabric. These blocks recorded significant bedding-parallel shearing, but the possibility that some blocks were olistoliths prior to deformation cannot be ruled-out.

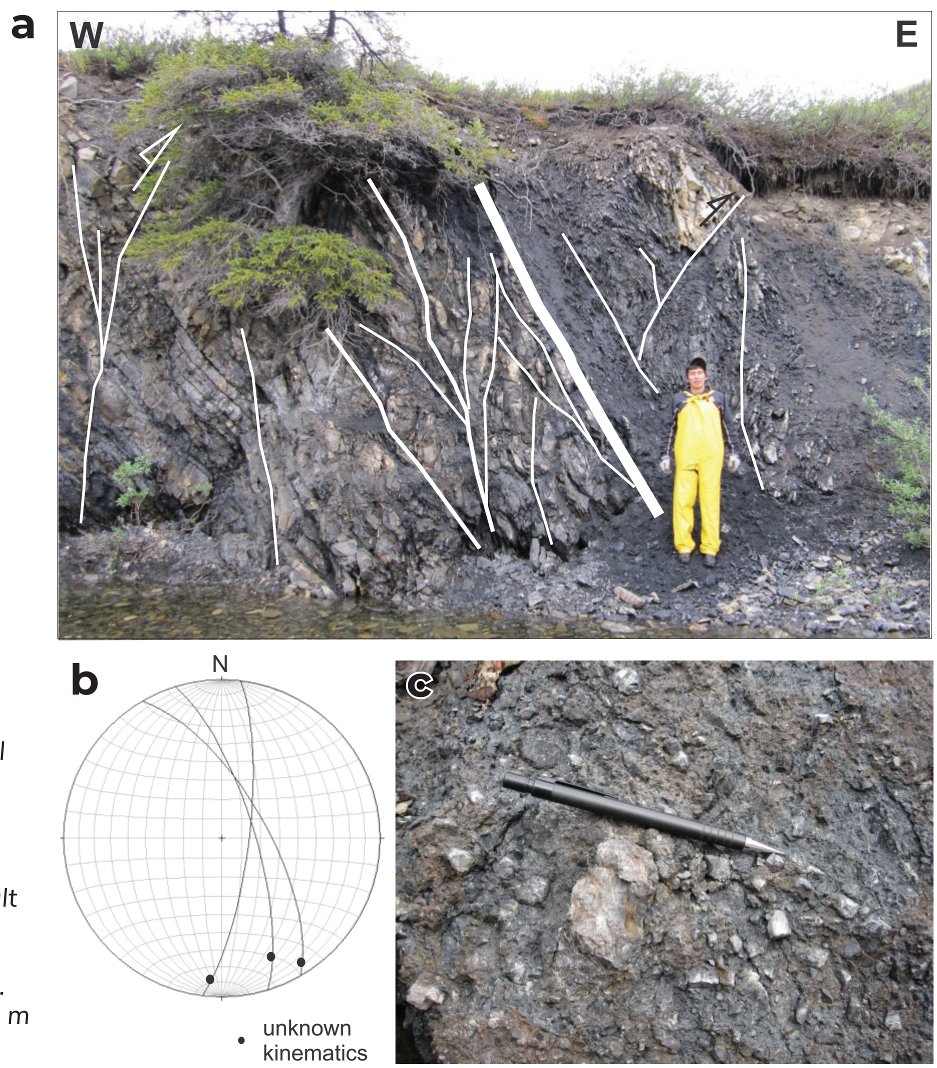

Figure 5. *West Tetlit fault (informal name). Location shown on section in Figure 4.* ***(a)*** *Highly deformed schistose zone.* ***(b)*** *Stereographic projection of fault planes found in the schistose zone; symbols on fault planes correspond to slickenlines.* ***(c)*** *Tectonic breccia located in the hanging wall of the schistose zone. The brecciated zone is around 120 m wide.*

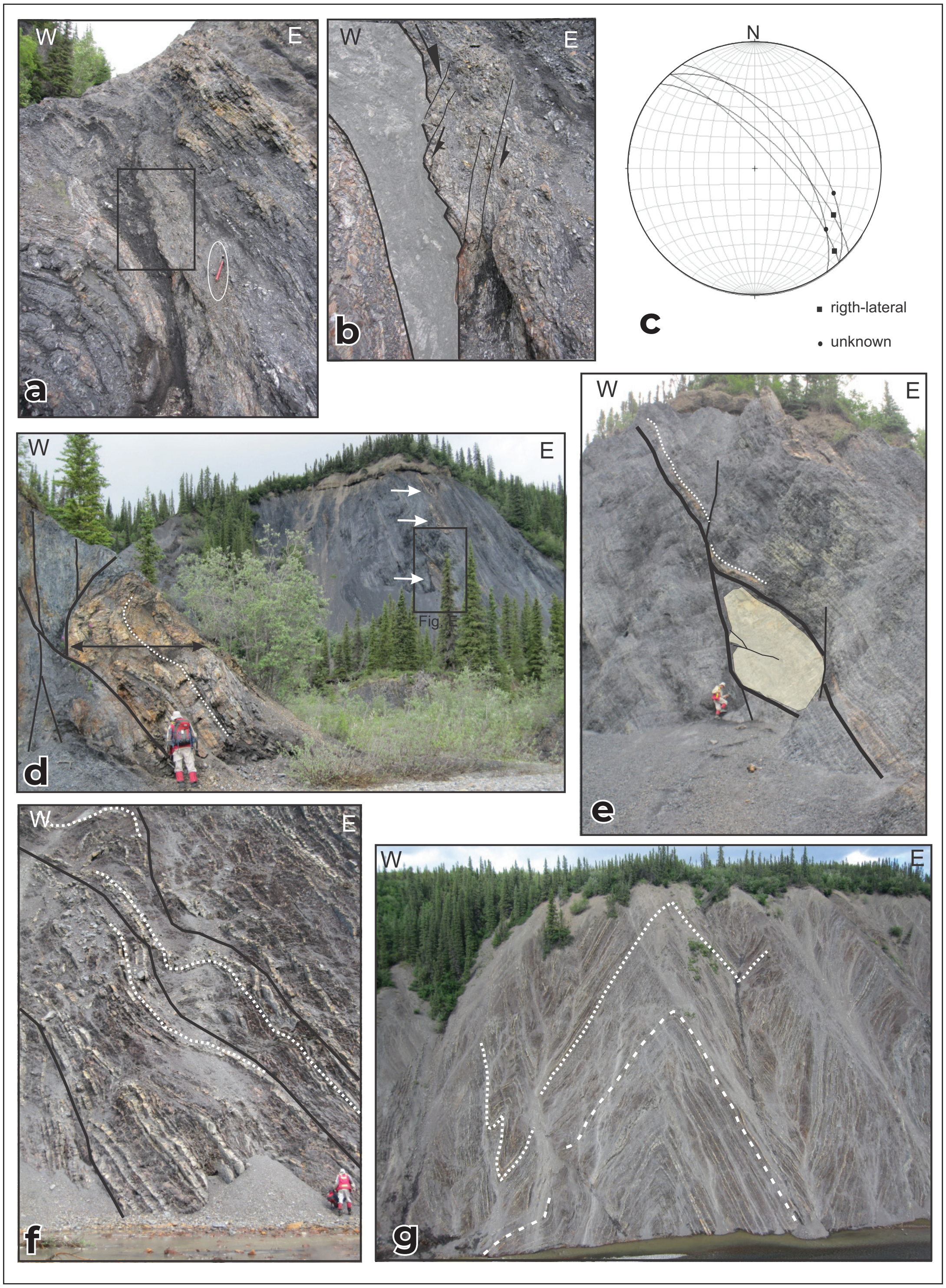

Figure 6. East Tetlit fault zone (informal name). Location on section in Figure 4. ***(a)*** Fault zone in the Canol Formation. Hammer for scale (outlined by white oval). ***(b)*** Close-up of area outlined in 6a. Slickensided surfaces, as well as minor Riedel-type second-order shears, indicate predominant right-lateral motion. ***(c)*** Stereographic projection of striated fault planes in the east Tetlit fault zone. Symbols on fault planes correspond to slickenlines. ***(d)*** Fault-bounded block (black arrows) in a shale-dominated interval. The white dotted line represents bedding. White arrows mark other fault-bounded blocks. ***(e)*** Close-up of fault-bounded block in a shale dominated assemblage in area outlined in 6d. The white dotted line represents bedding. Geologist for scale. ***(f)*** Faults subparallel to bedding. Note the fault-bend folds associated with change in the fault dip ('fault ramp'). Geologist for scale. ***(g)*** Upright chevron folds. The outcrop is approximately 40 m high.

West of the main deformation zone, the Imperial Formation exhibits numerous faults subparallel to bedding, and fault-bend folds are associated with change in the fault dip (Fig. 6f). The Imperial Formation also exhibits spectacular upright closed folds, hundreds of metres in wavelength, with angular hinge zones (Fig. 6g). The eastern fault within the east Tetlit fault zone corresponds to a steeply dipping deformation zone.

Second-order structural features in the footwall of the east Tetlit fault zone include brittle faults marked by deformation zones ranging in width from centimetres up to five metres (Fig. 4c). The orientations of slickenlines found on these second-order fault planes vary significantly suggesting a complete transition in time and/or space from faults with nearly downdip motion to strike-slip faults (Fig. 7). Faults having a normal component correspond to either discrete (Fig. 4d) or anastomosed features (Fig. 4b) allowing down-to-the-east motion. Folds are generally upright and wavelengths range from tens to hundreds of metres.

Deformation in the hanging wall of the east Tetlit fault zone corresponds to broad open folds involving the Imperial Formation (Allen, 2009; Fig. 4e).

Eastern Peel River section

Nearly continuous outcrops form a 5 km long section along the Peel River (Fig. 8; location 2 on Fig. 2) between the Knorr and Caribou faults of Norris (1981d). Due to the water level during fieldwork, most outcrops were not accessible. However, tectonic features are easily visible from several shoals in the riverbed.

Two main assemblages may be distinguished in the Road River Group: to the west, rocks consist of decimetre to metre thick layers of siltstone and limestone with shale intervals, whereas to the east, black shale predominates. The contact between fine-grained rocks belonging to the Carboniferous Ford Lake Shale that forms the eastern end of the studied section and the Road River Group is not exposed.

Folds are close to tight, and are overturned to the east (Fig. 8d). In the central part of the section, parasitic folds are asymmetric or 'S'-shaped, indicating that they belong to the western flank of a major syncline (Fig. 8a).

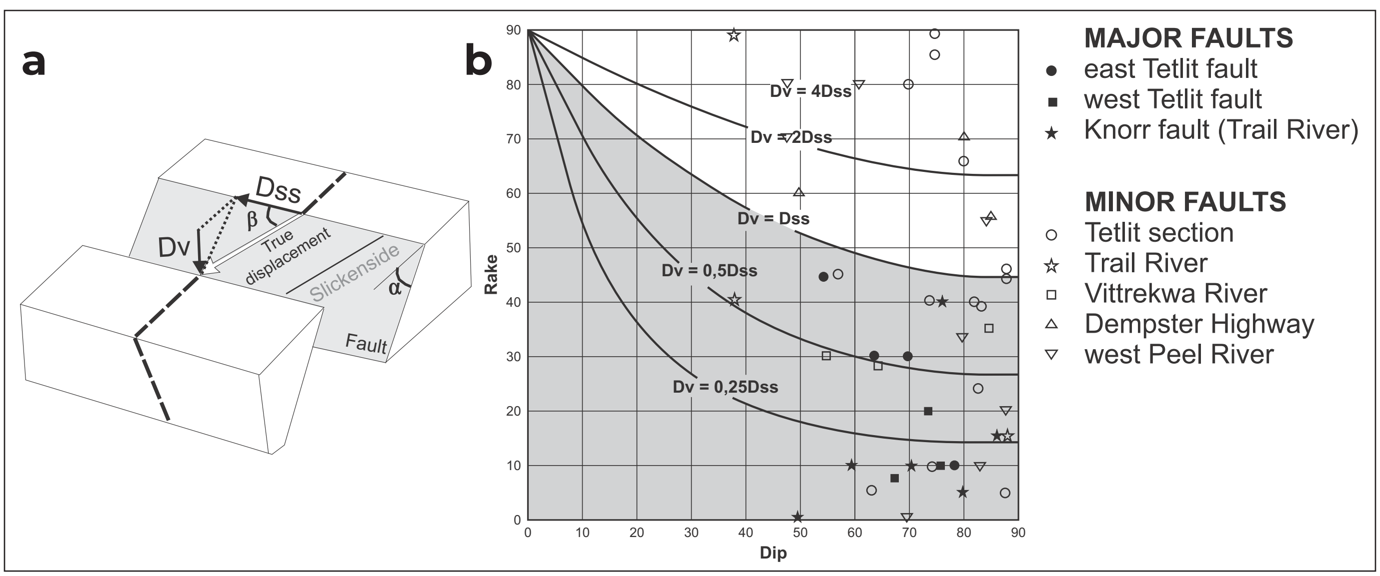

Figure 7. ***(a)*** *Relationship between the strike-slip (Dss) and vertical (Dv) components of displacement. α, dip of the fault plane; β, rake of the slickenline.* ***(b)*** *Diagram showing the kinematic of brittle faults based on fault dip and rake of slickenline. The field corresponding to faults with a predominant strike-slip motion (Dss>Dv) is shown in grey.*

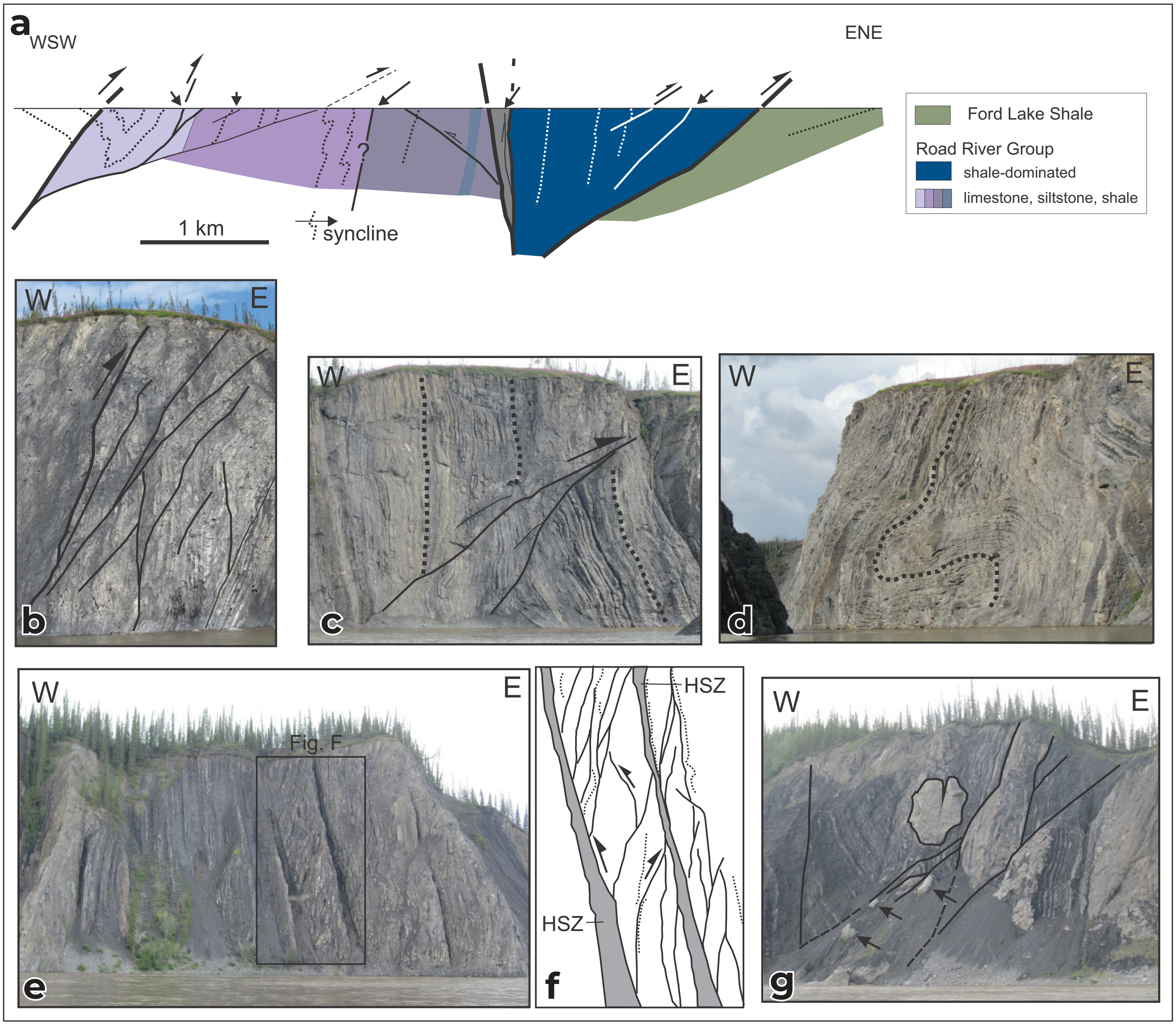

Figure 8. ***(a)*** *Cross section along the eastern Peel River (location 2 on Fig. 2). No vertical exaggeration. Arrows indicate the apparent sense of shear and do not take into account a potential strike-slip component.* ***(b)*** *Closely spaced steeply-dipping faults. Drag folds suggest apparent east-directed thrust motion along the faults.* ***(c)*** *Shallow-dipping faults recording apparent east-directed thrust motion.* ***(d)*** *Asymmetric east-verging folds.* ***(e)*** *Steeply dipping high-strain zone.* ***(f)*** *Sketch of the area outlined in 7e. The high-strain zone may record mainly strike-slip motion and cuts older second-order faults showing apparent east-directed thrust motion.* ***(g)*** *West-dipping faults, some of them bounding elongated more competent blocks (arrows).*

Moderate (30–40°; Fig. 8c) to steep (up to 70°; Fig. 8b) west-dipping faults are common along the Peel River section. Offset of marker beds and drag folds suggest east-directed thrusting. In the eastern part of the section, disconnected competent blocks are present in a shale-dominated assemblage (Fig. 8g). Shearing along block boundaries and faults cutting through the blocks attest to significant deformation.

A steep, east-dipping fault zone marked by several high-strain zones cuts west-dipping faults in the central part of the section (Fig. 8e,f). Based on the apparent dragging of the bedding and presence of west-dipping faults, the fault zone appears to be west-directed. However, the strike-slip component of motion may still predominate.

Trail River section

Along most of the studied segment of the Trail River section (Fig. 9; location 3 on Fig. 2), rock units dip toward the east, except close to a major fault zone that marks the northern extent of the Knorr fault of Norris (1981d). The conformable contact between the shale-dominated upper assemblage of the Road River Group and the Canol Formation is well exposed. The Imperial Formation overlies the Canol Formation to the east of the studied segment of the Trail River.

The main fault zone strikes ~N187 and corresponds to a steeply dipping, 10 m wide high strain zone that includes dismembered competent blocks in a fine-grained matrix. A brecciated zone, approximately 20 m in width and including subhorizontal to subvertical fracture planes, bounds the high strain zone to the east (Fig. 9d). Slickenlines found on second-order brittle fault planes indicate mainly right-lateral motion (Fig. 9e). This high strain zone (HSZ_2 on Fig. 9d) cuts a shallow dipping high strain zone (HSZ_1 on Fig. 9d) that divides two highly folded rock packages.

Second-order faults are common in the central part of the section (Fig. 9b,c) and include brittle structures showing either normal or thrust apparent motions. Bedding surfaces having slip indicators have been observed in several locations and are frequently cut by steeply dipping faults.

Vittrekwa River section

Within the studied section along the Vittrekwa River (location 4 on Fig. 2), the Imperial Formation dips steeply (average: 65–70°) generally toward the east. Brittle faults are common along the section and are generally steeply (>70°) dipping. High strain zones, one to three metres wide, parallel bedding, and record predominant right-lateral motions (Fig. 10). High strain zones are located in shale-rich intervals suggesting that beds were first tilted close to the vertical before strike-slip deformation in incompetent layers.

Shallow to moderately dipping (<50°) faults have been observed locally but their offsets and potential crosscutting relationships with high-angle faults remain unclear.

Dempster highway

The Trevor fault is partially exposed a few hundred metres north of the Dempster Highway (Fig. 11a; location 5 on Fig. 2). On the geological map of Norris (1981a), main structures trend N170 to N020 and put in contact the Upper Devonian Imperial Formation with Mesozoic rocks (attributed to the Jurassic North Branch Formation and Cretaceous Martin Creek Formation).

A north-trending deformation zone is well exposed in the eastern part of the section and separates a shale-dominated assemblage (Whitestone River Formation?) from locally micro-conglomeratic, grey, quartz-rich sandstones with a yellowish weathering colour (Kamik Formation?). The ~100 m deformation zone includes faults associated with decimetre-wide brecciated and/or schistose intervals with variable strikes and dips (Fig. 11b,d). Minor structures have no obvious pattern, but the slickenlines suggest two groupings (Fig. 11c). One group reflects mainly dip-slip motion on an array of subsidiary faults striking northwest. The other group indicates strike-slip motion on north-striking minor faults.

In the eastern part of the section, a fault-bounded block near the contact between the Mesozoic and Paleozoic assemblages attests to significant deformation. The fault that bounds the Imperial Formation toward the east is not exposed.

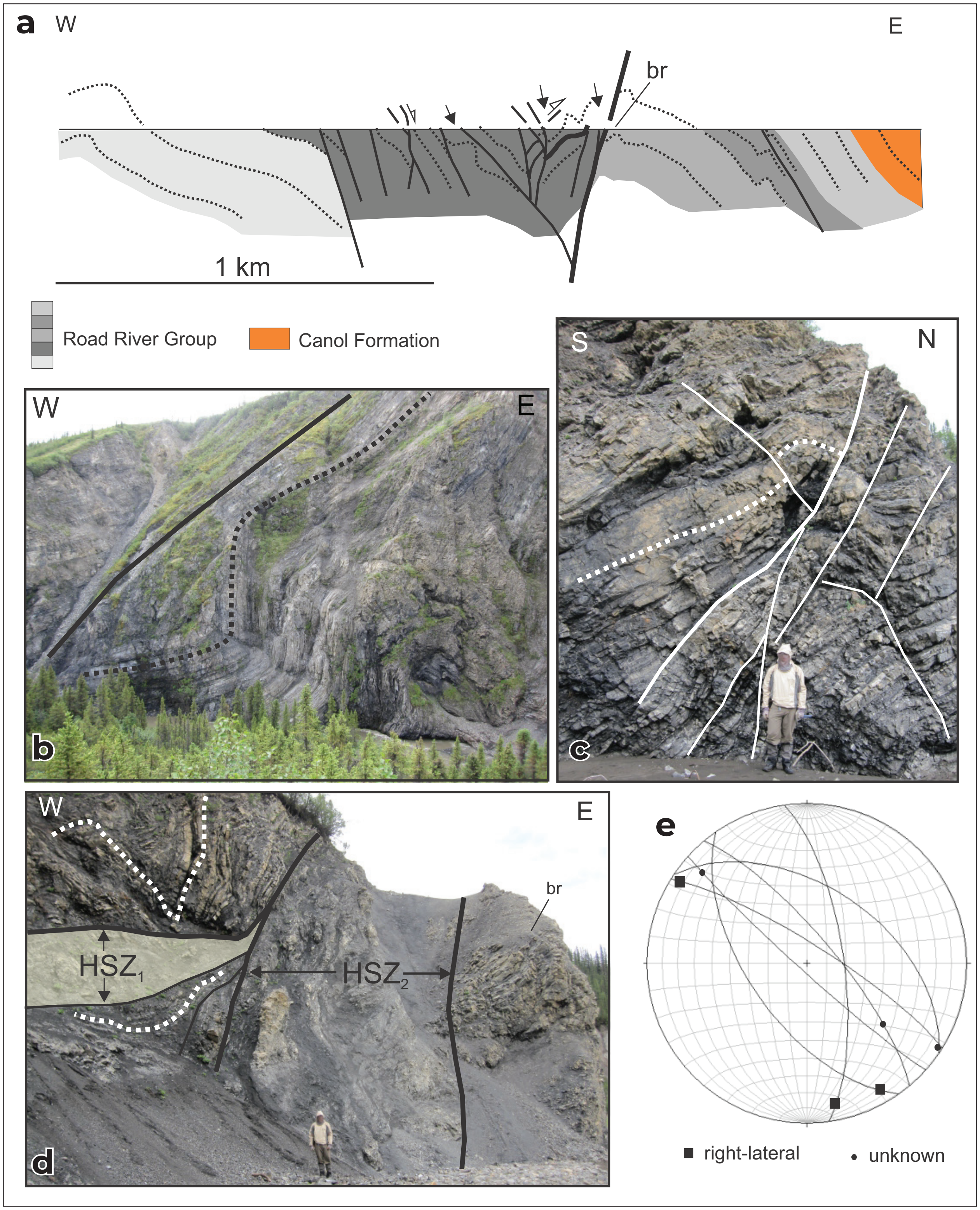

Figure 9. ***(a)*** *Cross section along the Trail River (location 3 on Fig. 2). No vertical exaggeration. Arrows indicate the apparent sense of shear and do not take into account a potential strike-slip component.* ***(b)*** *Asymmetric open fold;* ***(c)*** *second-order faults showing multiple cross-cutting relationships;* ***(d)*** *shallow-dipping high-strain zone (HSZ_1) cut by a steeply dipping high strain zone (HSZ_2) approximately 10 m wide. Rocks on the east side of HSZ_2 are brecciated (br); and* ***(e)*** *stereographic projection of striated fault planes found close to the HSZ_2. Symbols on fault planes correspond to slickenlines.*

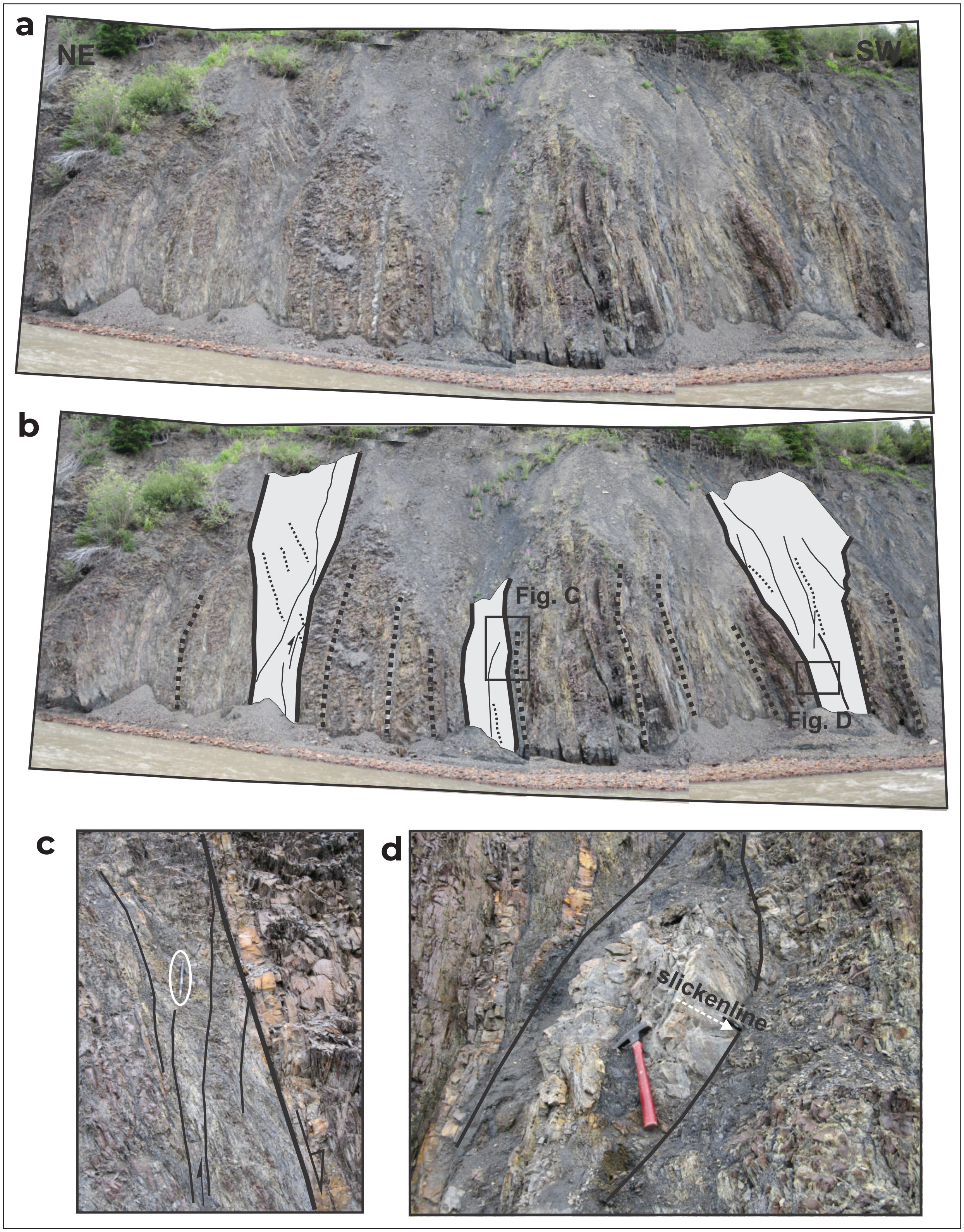

Figure 10. Vittrekwa River (location 4 on Fig. 2). ***(a and b)*** (with annotations), steeply dipping faults characterized by 1 to 3 m wide deformation zones (in white on 10b) parallel to bedding. ***(c)*** Close-up of second order synthetic faults within a deformation zone (area outlined in 10b). Arrows indicate the apparent sense of shear and do not take into account a potential strike-slip component. ***(d)*** Closer view of one of the few striated surfaces found in deformation zones and recording predominant right-lateral motion (area outlined in 10b).

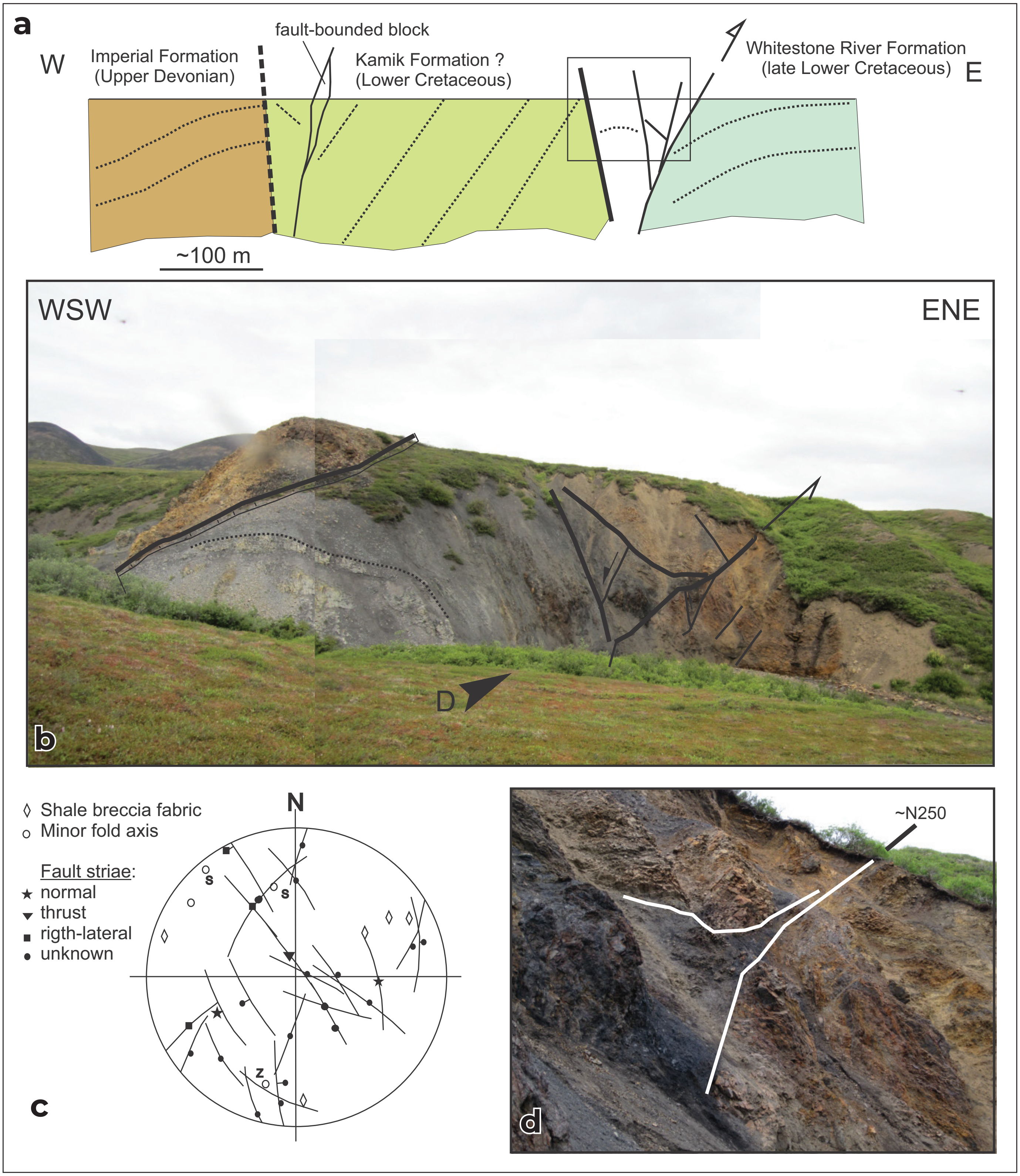

***Figure 11. (a)** Cross section of the fault zone along the Dempster Highway (location 5 on Fig. 2). **(b)** View of the eastern fault zone showing the variability of fault strikes. **(c)** Stereographic projection of striated second-order fault planes. Only part of great circles (fault planes) is shown. Symbols on fault planes correspond to slickenlines. **(d)** Closer view of a steeply dipping (around 70°) N250 trending fault (from point of view indicated in 11b).*

Western Peel River

In the Peel River area, the Deslauriers fault puts in contact the Slats Creek Formation to the west and the Road River Group to the east (Norris, 1981d). The fault zone is not exposed in the Peel valley. However, an elongated butte forms an isolated outcrop near or at the location of the Deslauriers fault, a few hundred metres south of the Peel River (location 6 on Fig. 2). The butte consists of a light grey weathered, erosion-resistant massive limestone. The limestone is brecciated, has fractures spaced at 10 to 50 cm, and has abundant neoformed calcite (Fig. 12a). Brittle fault planes have various orientations. However, continuous planes tend to strike parallel to the elongation of the butte, approximately N335, and correspond to left-lateral strike-slip faults (Fig. 12b).

Discussion

The east flank of the Richardson anticlinorium exhibits highly variable strain intensities. Along most of the studied sections, rock units dip shallowly to the east and are characterized by broad open folds, hundreds of metres in wavelength, and have few brittle structures attesting to low internal deformation. However, close to major faults, marked by deformation zones up to several hundred metres in width, rock units are steep and highly strained. Clear evidence of bedding-parallel shearing in steeply dipping shale-dominated assemblages is documented at several locations, including along the east Tetlit fault. The amount of displacement along bedding-parallel shears is difficult to quantify, but is probably significant.

A predominant dextral sense of motion is documented for several major faults belonging to the Richardson fault array (east Tetlit fault, Trail River fault, Vittrekwa River structures; Fig. 7). This is in agreement with previous studies that suggest that strike-slip faulting predominates (Jeletsky, 1961, 1975) and with Paleogene (?) dextral faults documented elsewhere in northern Yukon (von Gosen et al., 2019). The steep dip of major faults, as well as their kinematics, conflict with Hall and Cook's (1998) interpretation

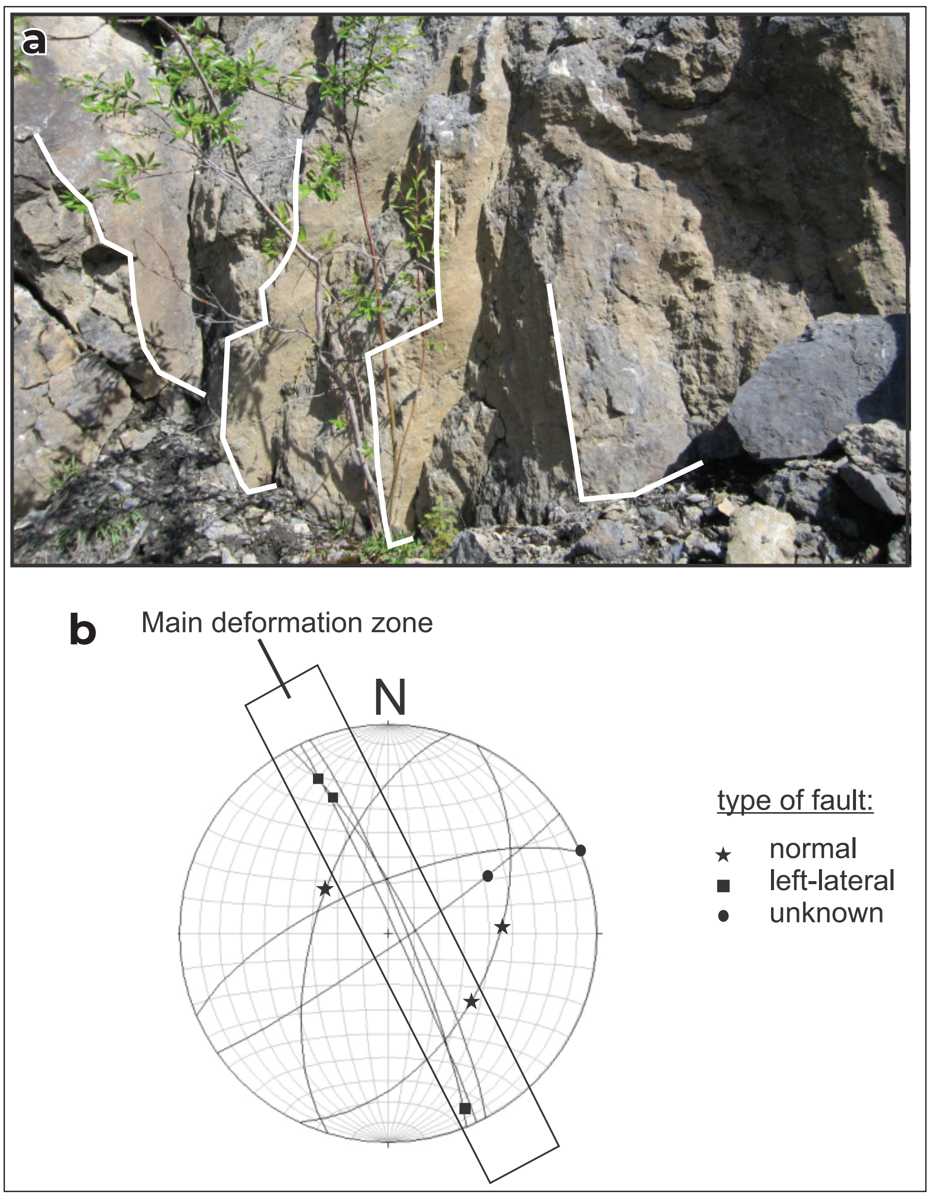

Figure 12. *Deslauriers fault near the Peel River (location 6 on Fig. 2).*
(a) *Closely spaced second-order fault planes (white lines).*
(b) *Stereographic projection of striated fault planes. Symbols on fault planes correspond to slickenlines.*

that the Richardson anticlinorium corresponds to a thrust-related pop-up structure formed above a regional detachment that roots westward beneath Eagle Plain.

Unambiguous evidence for left-lateral displacement has been documented along the Deslauriers fault (western Peel) in an elongated butte that corresponds to a tectonic block composed of limestone of uncertain age. This block may have experienced significant rotation and structures may have originally belonged to a group of N0 to N15 faults with left-lateral apparent displacements that have been mapped on the western flank of the Richardson anticlinorium (Norris, 1981b). Alternatively, these minor faults could belong to a distinct tectonic episode.

The Peel River section is characterized by a clear structural vergence toward the east. The significance of this change of deformation style in the southern Richardson Mountains is uncertain.

Second-order faults exhibit highly variable kinematics (Fig. 7) and both normal and thrust faults have been documented. In several cases (e.g., sections along the eastern Peel, Trail and Vittrekwa rivers), strike-slip faults cut more shallow dipping faults and/or follow steep bedding planes, suggesting that dextral motions affected a previously tilted and deformed sedimentary succession. However, crosscutting relationships are rare and it is unclear whether the various faults were active during a single progressive phase or several discrete deformation episodes. Polyphase deformation may explain the scattered distribution of bedding orientations.

Cecile (1984) used the apparent offset of the Canol Formation to estimate a less than 20 km displacement along the RFA. On the western flank of the Richardson Mountains, the Canol Formation has a clear geomorphologic signature (Norris, 1981b) and offset estimates are likely reliable. On the east flank, however, the signature is more subtle and the mapped location of the Canol Formation is more ambiguous. In addition, structural repetitions (such as the one observed on the Tetlit section) may contribute to the geometrical complexity on the eastern flank of the Richardson anticlinorium, which renders any displacement estimate highly uncertain.

However, the deformation documented in fault zones exhibits several characteristics (including width) generally associated with faults that experienced significant displacements. As such, possible large offset on the eastern flank of the Richardson anticlinorium should be considered along with independent evidence (present day seismicity; relatively steep gravity gradients; large wavelength magnetic anomaly pattern) that suggests the presence of regional-scale structure(s).

Consequently, the traditional interpretation of Paleozoic and Mesozoic succession thickness and facies variations essentially resulting from a complex paleogeography warrants further investigation. Such an interpretation may have led to invalid and/or imprecise palinspastic reconstructions because sedimentary rocks from distinct settings may have been tectonically juxtaposed along major faults.

Acknowledgements

This study was conducted as part of a GEM project led by Larry Lane; I thank him for giving me the opportunity to do some fieldwork. Tammy Allen shared her expertise on northern Yukon geology. Miranda Charlie, Yudii Mercredi and Adam Hayman provided valuable field assistance. This paper has been improved by the reviews of Sébastien Castonguay and Maurice Colpron. This is GSC contribution No. 20200527.

Reference

Allen, T.L., 2009. Field notes on the Upper Devonian Imperial Formation (NTS map sheet 106L), Tetlit Creek, east Richardson Mountains, Yukon. *In*: Yukon Exploration and Geology 2009, K.E. MacFarlane, L.H., Weston and L.R. Blackburn (eds), Yukon Geological Survey, p. 1–21.

Cecile, M.P., 1984. Evidence against large-scale strike-slip separation of Paleozoic strata along the Richardson-Hess fault system, northern Canadian Cordillera. Geology, vol., 12, p. 403–407.

Crawford, B.L., Betts, P.G. and Aillères, L., 2010. An aeromagnetic approach to revealing buried basement structures and their role in the Proterozoic evolution of the Wernecke Inlier, Yukon Territory, Canada. Tectonophysics, vol. 490, p. 28–46.

Dixon, J., 1996. Cretaceous and Tertiary. *In*: Geology and mineral and hydrocarbon potential of northern Yukon Territory and northwestern district of Mackenzie. Geological Survey of Canada, Bulletin 422, p. 301–317.

Eisbacher, G.H., 1983. Devonian-Mississippian sinistral transcurrent faulting along the cratonic margin of western North America: A hypothesis. Geology, vol. 11, p. 7–10.

Fraser, T.A. and Hutchison, M.T., 2017. Lithogeochemical characterization of the Middle-Upper Devonian Road River Group and Canol and Imperial formations on Trail River, eastern Richardson Mountains, Yukon: age constraints and a depositional model for fined-grained strata in the Lower Paleozoic Richardson trough. Canadian Journal Earth Sciences, vol. 54, p. 731–765.

Hall, K.W. and Cook, F.A., 1998. Geophysical transect of the Eagle Plains foldbelt and Richardson Mountains anticlinorium, northwestern Canada. Geological Society of America Bulletin, vol. 110, p. 311–325.

Jeletzky, A., 1961. Eastern slope, Richardson Mountains: Cretaceous and Tertiary structural history and regional significance. *In:* Geology of the Arctic, Volume I: University of Toronto Press, p. 532–583.

Jeletzky, J.A., 1975. An estimate of right-lateral displacement on Donna River Fault, northwestern district of Mackenzie, NWT Geological Survey of Canada, Paper 75-1, Part A, p. 541–543.

Lane, L.S., 1998. Latest Cretaceous-Tertiary tectonic evolution of northern Yukon and adjacent Arctic Alaska. American Association Petroleum Geologist Bulletin, vol. 82, p. 1353–1371.

Mazotti, S. and Hyndman, R.D., 2002. Yakutat collision and strain transfer across the northern Canadian Cordillera. Geology, vol. 30, p. 495–498.

Morrow, D.W., 1999. Lower Paleozoic stratigraphy of northern Yukon Territory and northwestern district of Mackenzie. Geological Survey of Canada, Bulletin 538, 202 p.

Norford, B.S., 1996. Ordovician and Silurian. *In*: Geology and mineral and hydrocarbon potential of northern Yukon Territory and northwestern district of Mackenzie. Geological Survey of Canada, Bulletin 422, p. 119–162.

Norris, D.K., 1981a. Geology, Fort McPherson, District of Mackenzie. Geological Survey of Canada, A-series map 1520A, scale 1:250 000.

Norris, D.K., 1981b. Geology, Eagle River, Yukon Territory. Geological Survey of Canada, A-series map 1523A, scale 1:250 000.

Norris, D.K., 1981c. Geology, Trail River, Yukon-Northwest Territories. Geological Survey of Canada, A-series map 1524A, scale 1:250 000.

Norris, D.K., 1981d. Geology, Wind River, Yukon Territory. Geological Survey of Canada, A-series map 1528A, scale 1:250 000.

Norris, D.K., 1985. Eastern Cordillera foldbelt in northern Canada: its structural geometry and hydrocarbon potential. American Association of Petroleum Geologists Bulletin, vol. 69, p. 788–808.

Norris, D.K., 1996. Physiographic setting. *In:* Geology and mineral and hydrocarbon potential of northern Yukon Territory and northwestern district of Mackenzie. Geological Survey of Canada, Bulletin 422, p. 7–20.

Norris, D.K. and Hopkins, W.S., 1977. The geology of the Bonnet Plume Basin, Yukon Territory. Geological Survey of Canada, Paper 76-8, 20 p.

Norris, D.K. and Yorath, C.J., 1981. The North American Plate from Arctic Archipelago to the Romanzof Mountains. *In*: The Arctic Ocean, A.E. Nairn, M. Churkin Jr. and F.G. Stehli (eds.), Springer Science + Business Media, New York, p. 37–103.

Osadetz, K.G., Chen, Z. and Bird, T.D., 2005. Petroleum Resource Assessment, Eagle Plain Basin and Environs, Yukon Territory, Canada. Yukon Geological Survey Open File 2005-2, Geological Survey of Canada, Open File 4922, 88 p.

Pugh, D.C., 1983. Pre-Mesozoic geology in the subsurface of the Peel River map area, Yukon Territory and district of Mackenzie. Geological Survey of Canada, Memoir 401, 61 p.

Rohr, K.M.M., Lane, L.S. and MacLean, B., 2011. Subsurface compressional structures and facies transitions imaged by seismic reflection data, eastern margin of Richardson Trough, Peel Plateau, Yukon. Bulletin of Canadian Petroleum Geology, vol. 59, p. 131–146.

Strauss, J.V., Fraser, T., Melchin, M.J., Allen, T.J., Malinowski, J., Feng, X., Taylor, J.F., Day, J., Gill, B.C. and Sperling, E.A., 2020. The Road River Group of northern Yukon, Canada: early Paleozoic deep-water sedimentation within the Great American Carbonate Bank. Canadian Journal Earth Sciences, vol. 57, p. 1193–1219.

von Gosen, W., Piepjohn, K., McClelland, W.C. and Colpron, M., 2019. Evidence for the sinistral Porcupine shear zone in North Yukon (Canadian Arctic) and geotectonic implications. *In:* Circum-Arctic Structural Events: Tectonic Evolution of the Arctic Margins and Trans-Arctic Links with Adjacent Orogens, K. Piepjohn, J.V. Strauss, L. Reinhardt, and W.C. McClelland (eds.), Geological Society of America, Special Paper 541, p. 473–491.